Purdue University
Purdue e-Pubs

Birck and NCN Publications | Birck Nanotechnology Center

8-1-2012

A Batch-Fabricated Single-Layer Elastomeric Actuator With Corrugated Surface

Teimour Maleki
Purdue University, Birck Nanotechnology Center, tmalekij@purdue.edu

Girish Chitnis
Purdue University, Birck Nanotechnology Center, gchitnis@purdue.edu

Albert Kim
Purdue University, Birck Nanotechnology Center, kim126@purdue.edu

Babak Ziaie
Purdue University, Birck Nanotechnology Center, bziaie@purdue.edu

Follow this and additional works at: http://docs.lib.purdue.edu/nanopub

Part of the Nanoscience and Nanotechnology Commons

Maleki, Teimour; Chitnis, Girish; Kim, Albert; and Ziaie, Babak, "A Batch-Fabricated Single-Layer Elastomeric Actuator With Corrugated Surface" (2012). *Birck and NCN Publications.* Paper 880.
http://docs.lib.purdue.edu/nanopub/880

This document has been made available through Purdue e-Pubs, a service of the Purdue University Libraries. Please contact epubs@purdue.edu for additional information.

A Batch-Fabricated Single-Layer Elastomeric Actuator With Corrugated Surface

Teimour Maleki, *Member, IEEE*, Girish Chitnis, Albert Kim, and Babak Ziaie, *Senior Member, IEEE*

***Abstract*—In this paper, we report on the first laser-micromachined batch-fabricated single-layer elastomeric actuator with a corrugated surface profile. The structural material of the cantilever actuator is a single [polydimethylsiloxane (PDMS)] layer, and electrodes are soft lithographically patterned conductive carbon grease. The asymmetric corrugated surface provides a bending moment in a single PDMS layer without the need for a second inactive layer. An actuator which is 5 mm long, 1 mm wide, and 80 μm thick can generate up to 2-mm out-of-plane displacement with zero applied force and 15 μN at zero deflection while consuming 20 μW of static power when actuated with 500 V. [2011-0159]**

***Index Terms*—Carbon grease, elastomeric actuators, electrostrictive polymers, laser micromachining, polydimethylsiloxane (PDMS).**

I. Introduction

LOW-COST lightweight out-of-plane actuators are indispensable elements in a variety of robotics and biomedical applications [1]–[4]. Electrostatic, magnetic, thermal, pneumatic, piezoelectric, and several other actuation mechanisms, each with their unique advantages and disadvantages, have been used to implement such actuators [5]–[14]. Dielectric elastomer (DE) actuators are a new emerging class of electromechanical transducers with exceptional properties such as large strains, fast response, high efficiency/performance, low cost, high fracture toughness, and inherent vibration damping [15]–[18]. These properties enable DE actuators to be a potential candidate in large range of applications including artificial muscle, microelectromechanical systems (MEMS), smart skin, and haptic displays [19]–[21]. One drawback of DE actuators is their high actuation voltages (in the kilovolt range). Several groups have attempted to address this issue (i.e., reducing the actuation voltage or increasing the strain for a given voltage) by various means such as modification of material properties, engineering new materials, improving electrode geometry, and mechanical contraptions such as film prestretching [22]–[27]. Additional difficulty concerning DE actuators is their nonbatch-mode fabrication process. Most out-of-plane DE actuators are handmade, use several structural layers, and have complicated fabrication processes. In this paper, we focus on developing a new structure for an out-of-plane DE actuator using a single-layer elastomer with a corrugated surface to overcome difficulties in batch fabrication and multilayer integration. Geometric design of the actuator makes single-layer implementation possible; in fact, the described device is the only reported single-layer DE actuator. In addition, laser micromachining in combination with soft lithography is used to achieve a batch-scale fabrication process. In Section II, we describe the actuator design and simulation. Section III elaborates on the fabrication process followed by measurement results in Section IV. Finally, in Section V, we conclude by summarizing our efforts and suggest several areas for further investigation.

Manuscript received May 22, 2011; revised February 8, 2012; accepted March 14, 2012. Date of publication April 26, 2012; date of current version July 27, 2012. Subject Editor F. Ayazi.

T. Maleki and A. Kim are with the Birck Nanotechnology Center, Purdue University, West Lafayette, IN 47907 USA (e-mail: tmalekij@purdue.edu; kim126@purdue.edu).

G. Chitnis is with Purdue University, West Lafayette, IN 47907 USA (e-mail: gchitnis@purdue.edu).

B. Ziaie is with the School of Electrical and Computer Engineering, Purdue University, West Lafayette, IN 47907 USA (e-mail: bziaie@purdue.edu).

Color versions of one or more of the figures in this paper are available online at http://ieeexplore.ieee.org.

Digital Object Identifier 10.1109/JMEMS.2012.2192909

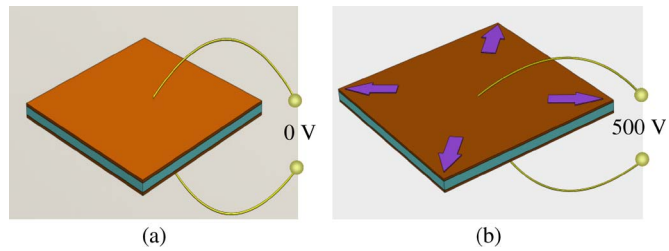

Fig. 1. Operation principle of dielectric elastomeric actuators. (a) Relaxed state. (b) Actuated through application of a voltage to the compliant electrodes.

II. Design and Simulation

Dielectric elastomeric actuators consist of a soft material (polydimethylsiloxane (PDMS) in our design) sandwiched between two conductive and compliant electrodes (carbon grease in our design) (Fig. 1) [28]. When there is no voltage across the electrodes, the soft material is in a relaxed state [Fig. 1(a)]. Applying a voltage across the compliant electrodes induces an electrostatic pressure that squeezes the soft elastomer, reducing its thickness and increasing its lateral dimensions [Fig. 1(b)] because the elastomer has a Poisson's ratio close to 0.5 and keeps its volume constant during deformation.

A single-layer elastomeric cantilever would bend in an out-of-plane direction if asymmetric stresses are applied to its top and bottom surfaces. This asymmetric stress profile can be achieved through geometric design of the surfaces. Fig. 2 shows 3-D schematic and cross section of a single-layer elastomeric cantilever actuator with such an asymmetric surface profile, i.e., the top surface is corrugated, while the bottom one is flat. This surface profile is designed such that the thickness (d) of the actuator is changing periodically [Fig. 2(b)]. The

1057-7157/$31.00 © 2012 IEEE

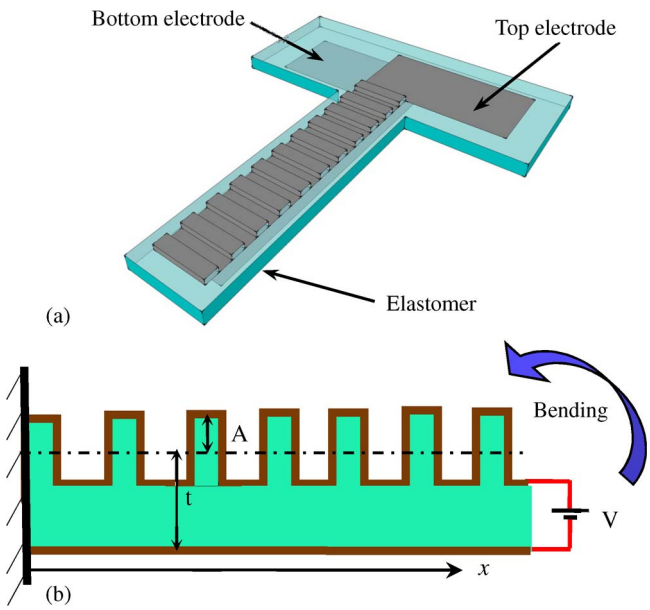

Fig. 2. (a) Three-dimensional schematic and (b) cross-sectional view of a single-layer elastomeric actuator with an asymmetric surface profile.

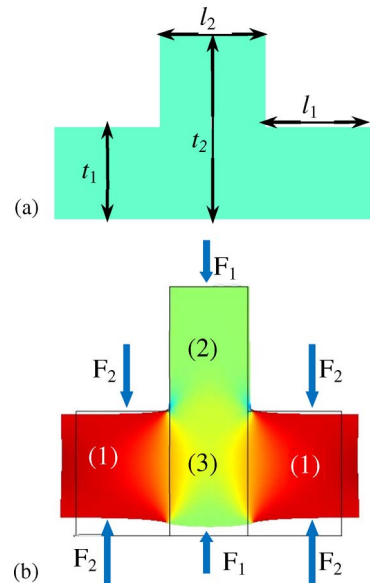

Fig. 3. Simplified structure of one element of the asymmetric actuator. (a) Without applied voltage. (b) With applied actuation voltage inducing a bending moment in the element.

structure thickness can be thought of as a superposition of two components, a constant term (t) with a square wave (magnitude A and frequency ω) superposition representing the corrugation. When a constant voltage is applied across top and bottom electrodes, the resulting transverse stress in the elastomer can be approximated as

$$\sigma = -\frac{1}{2}\varepsilon\varepsilon_0 \frac{V^2}{(t \pm A)^2} \tag{1}$$

where ε is the elastomer dielectric constant, ε_o is the air permeability, and V is the applied voltage. The asymmetric surface profile induces a nonuniform transverse compression and longitudinal expansion, resulting in a bending moment in the cantilever.

In order to better understand the actuation mechanism, a simplified structure is shown in Fig. 3. Induced electrostatic force is assumed to be perpendicular to the surface of the actuator in this simplified model. A single actuator unit without any actuation voltage is shown in Fig. 3(a), while similar unit after actuation is shown in Fig. 3(b). Color change illustrates the simulated induced compressive stress in the thinner segment which is larger compared to that of the thicker part. Although (1) predicts a uniform stress across both the thinner and thicker segments, we hypothesize that part of the thicker segment (region 3) connected to the thinner one (region 1) experiences higher stress values as a result of the transferred stress from the adjoining thinner regions [Fig. 3(b)]. Associated with the transverse stress is a considerable longitudinal one due to high value of PDMS Poisson's ratio (~0.5). As shown in Fig. 2(b), a higher longitudinal strain in the bottom part of the cantilever results in more elongation along X-axis compared to the top part, deflecting the cantilever in the upward direction.

To confirm our hypothesis, Comsol Multiphysics was used to simulate the stress/strain in the simplified structure shown in Fig. 3, using PDMS as elastomeric material ($Young's\ modulus = 750$ kPa; $Poisson's\ ratio = 0.49$; *dielectric constant*, $\varepsilon = 2.7$). To avoid any rigid body motion during the simulation, two nodes were fixed as shown in Fig. 4(a).

Simulation results are summarized in Fig. 4. Fig. 4(b) shows the stress (σ_y) along several cross sections of the beam shown by red lines in Fig. 4(a). Difference in stress levels in the top and bottom sections of the thick part is evident from the plot. Due to Poisson's effect, higher stress (σ_y) results in greater strain levels along X-direction (ε_x) which is depicted in the color plot [Fig. 4(a)]. This is similar to a bimaterial beam in which a given temperature difference results in dissimilar expansions and bending. However, in case of the PDMS actuator presented here, dissimilarity in expansion is achieved by geometric design and applied voltage. One can notice a very slight upward deflection of the bottom right corner in Fig. 4(a). Although this deflection is very small for a single element, if multiple elements are used, it is expected to add up, resulting in a significantly larger movement. Such multielement PDMS cantilever (5 mm long and 1 mm wide) was used for parametric study. The effect of element size [variations in $l_1, l_2, t_1,$ and t_2 as shown in Fig. 3(a)] on the deflection was simulated without changing the overall size of the cantilever. Fig. 4(c) shows one such case ($l_1 = 60$ μm, $l_2 = 20$ μm, $t_1 = 40$ μm, and $t_2 = 100$ μm). Inset in the figure clearly shows nonuniform stresses as expected which shows that our analysis based on single element can be extended to multielement structure.

Fig. 5 shows the deflection simulation results versus thick segment's length [l_2 in Fig. 3(a)] for a 5-mm-long 1-mm-wide actuator when 1-kV voltage is applied. In this simulation, the thickness of the thin segment [t_1 in Fig. 3(a)] and the whole element length $(l_1 + l_2)$ are kept fixed at 40 and 80 μm, respectively. As can be seen, deflection is increasing with larger l_2/l_1 ratio. This can be explained by the fact that the induced deflection is mostly due to an asymmetric strain in the thicker segment [see Fig. 4(b)], and the length of the thin segment

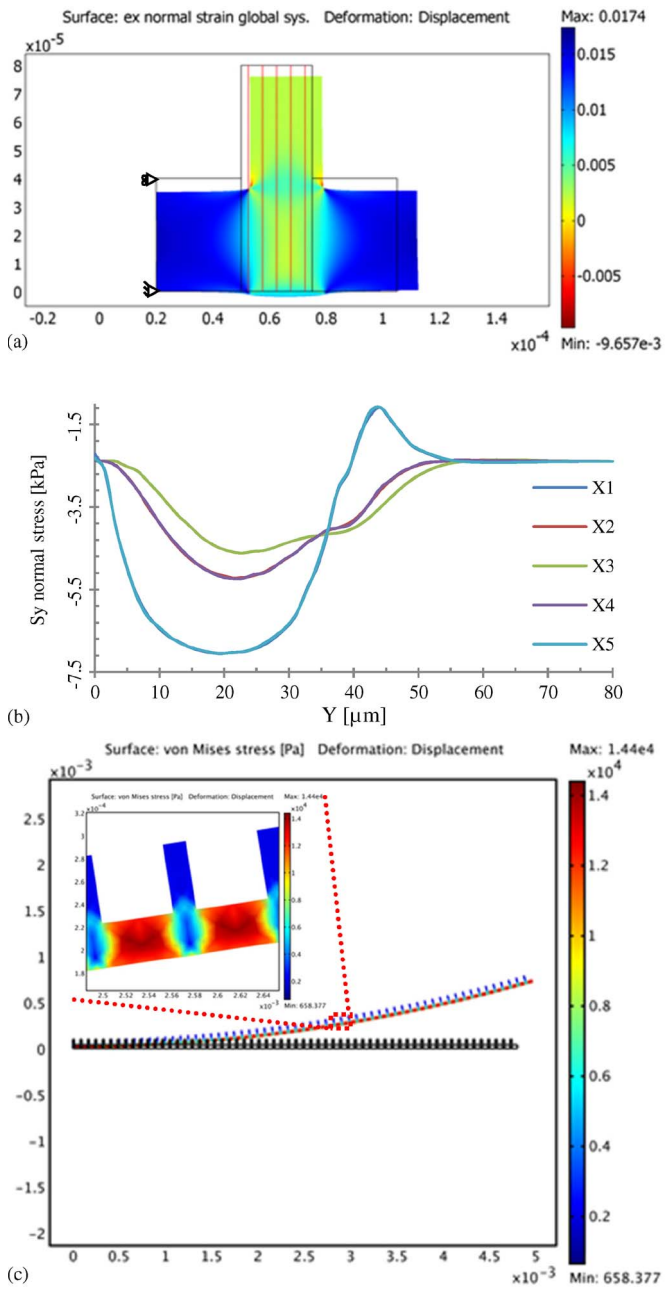

Fig. 4. Comsol simulation of a single element of the actuator. (a) Nonuniform displacement. (b) Normal stress along (shown by red lines) multiple cross sections. (c) Comsol simulation results for the 5-mm-long asymmetric actuator. Inset clearly shows nonuniform induced stress in the thicker segment.

has limited effect on the deflection. Therefore, the longer the thick segment, the higher the deflection. The inset in Fig. 5 shows deflection versus thick segment thickness t_2, while l_1, l_2, and t_1 are held constant at 5, 75, and 40 μm, respectively. As illustrated in the figure, deflection is higher for an actuator with increased thick segment thickness, due to the minimal effect of thin segment on the asymmetry of the induced longitudinal strain.

Simulation results for deflection versus thick segment length for 5-mm-long and 1-mm-wide actuators having different thin segment thicknesses t_1 are shown in Fig. 6. In this simulation, the thickness of the thick segment t_2 is assumed to be fixed at 100 μm. As shown in the figure, the thinner the

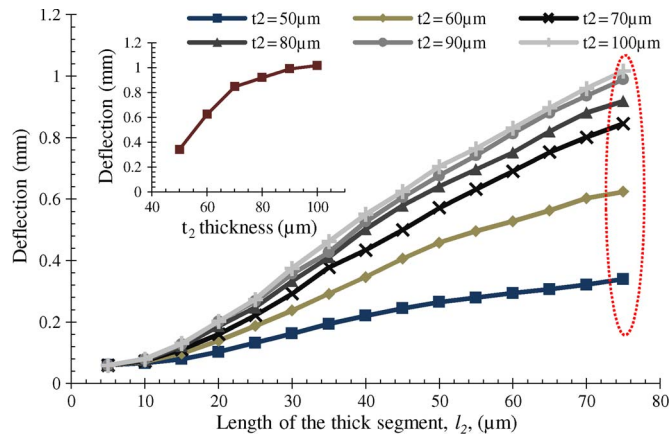

Fig. 5. Simulation results for asymmetric actuators showing tip deflection versus the length of the thick segment (t_2 as the variable parameter). (Inset) Deflection versus the thickness of the thicker segment with other parameters kept constant (see the text).

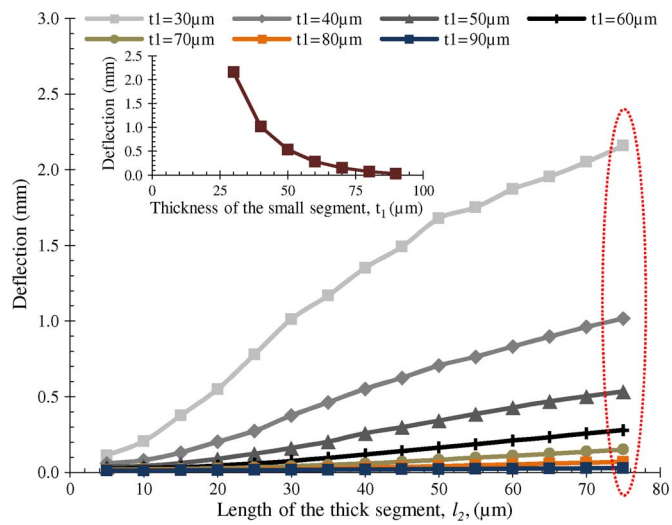

Fig. 6. Simulation results for asymmetric actuators showing tip deflection versus the length of the thick segment (t_1 as the variable parameter). (Inset) Deflection versus the thickness of the thinner segment with other parameters kept constant (see the text).

thin segment, the higher the deflection. This is because of the higher transverse contraction [see (2)] in the thin segment. The inset of the figure represents the deflection versus thin segment thickness t_1, while l_1, l_2, and t_2 are 5, 75, and 100 μm, respectively.

In another set of simulations, the reaction force at the tip (with zero displacement) versus the length of the thick segment was calculated (the thin and thick segment thicknesses were kept constant at 40 and 100 μm, respectively) (Fig. 7). As can be seen, an actuator with a longer thick segment creates less force. This is due to the fact that longer segment can dissipate nonsymmetrical strain in itself, hence creating smaller force than that of an actuator with shorter segment length.

In conclusion, simulation results suggest that an actuator with a very asymmetric profile (large l_2/l_1 and t_2/t_1) generates maximum deflection. However, such an actuator would generate least amount of force. We should mention that practical limitations might prevent the fabrication of such structures.

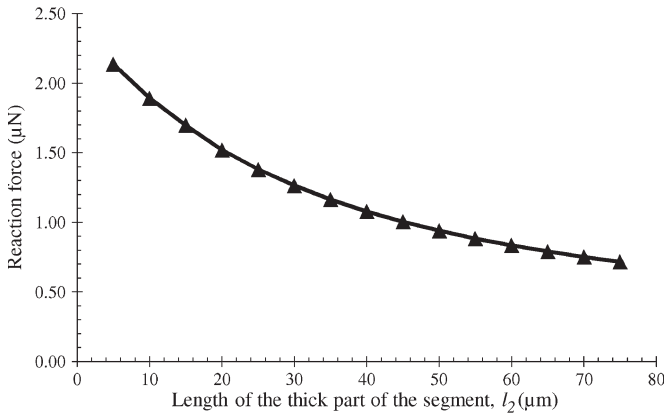

Fig. 7. Reaction force at the end of cantilever actuator versus the length of the thicker region with other parameters fixed (see the text).

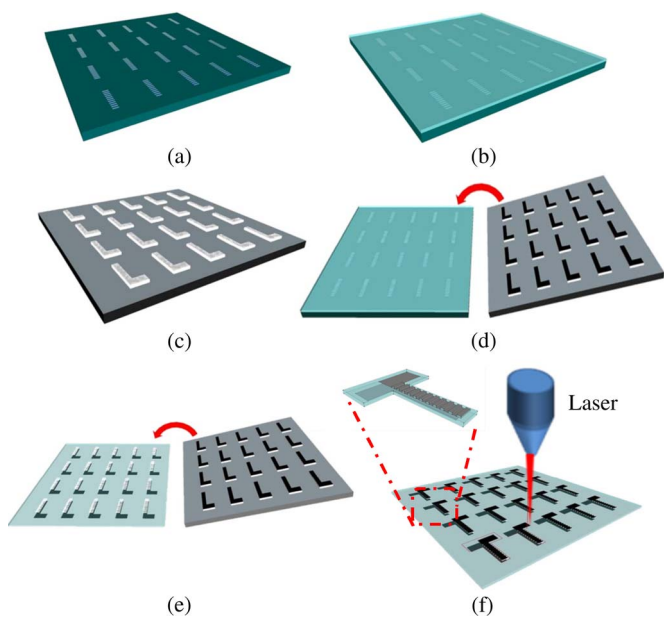

Fig. 8. Batch-scale fabrication process of the elastomeric actuators: (a) Etched silicon mold, (b) PDMS casting for the actuator, (c) PDMS stamp for the electrodes fabricated from an SU-8 mold, (d) stamping the electrodes on the actuator's flat surface, (e) stamping the electrodes on the corrugated surface, and (f) batch-scale separation with laser micromachining.

For example, achieving a uniform electrode coating is very difficult in an actuator with very narrow and deep surface nonuniformity. Moreover, handling ultrathin PDMS sheets (less than 40 μm) is another challenge in fabricating such an actuator. In the following sections, fabrication and experimental results for an actuator with the following geometrical parameters are presented: $l_1 = 20$ μm, $l_2 = 70$ μm, $t_1 = 40$ μm, and $t_2 = 100$ μm.

III. Fabrication Process

A batch-compatible fabrication process for the elastomeric actuator using PDMS as the structural material and conductive grease as the electrodes is shown in Fig. 8. PDMS was chosen as the structural material due to its well-known mechanical/electrical properties, low cost, and MEMS-compatible fabrication processability, while good adhesion to the structural material (PDMS) and low deformation resistance were reasons behind choosing conductive carbon grease as the electrode material. The process starts with the fabrication of a silicon mold with a corrugated top surface (60 μm deep) using isotropic silicon wet etching in HNA (20%wt HF:70%wt HNO_3: 10%wt CH_3COOH) [Fig. 8(a)]. Next, a 100-μm-thick PDMS (SYLGARD 184, Dow Corning, Midland, MI, mixing ratio $= 10 : 1$) is spun coated (1500 r/min for 30 s) and cured (at 120 °C for 30 min) to form the structural layer with asymmetric surface profile [Fig. 8(b)].

Separately, another SU8 (Microchem Corporation, MA, USA) mold is prepared using regular photolithography, and a PDMS stamp is fabricated by casting against the SU-8 mold [Fig. 8(c)]. The PDMS stamp is then inked by conductive carbon grease (846-80G, MG Chemicals, Burlington, Ontario, CA; electrical resistivity $= 0.01\ \Omega \cdot$ cm; density $= 2.7$ g/ml) and is used to deposit the top electrode on the PDMS structural layer (on the noncorrugated side) [Fig. 8(d)]. Subsequently, the stamped PDMS layer is transferred to a parylene-coated acrylic sheet in such a manner that the stamped surface is faced against the parylene (carbon grease has low adhesion to parylene, thus preventing transference of the electrode to the parylene surface). Afterward, aligned stamping of the top electrode on the corrugated surface is performed [Fig. 8(e)]. A slight pressure is necessary during stamping the top electrode on the corrugated surface in order to deform the nonplanarity and ensure a uniform coverage. Finally, laser micromachining (CO_2 laser, 2007 Professional Systems, Universal Laser System, AZ, USA) is used to separate the individual actuators at the wafer level [Fig. 8(f)].

A photograph of an array of the batch-fabricated actuators on the acrylic sheet prior to laser micromachining is shown in Fig. 9(a). SEM image of the corrugation on the surface of the actuator after electrode stamping illustrating the uniform coverage of the corrugated surface by carbon grease is shown in Fig. 9(b). An optical micrograph of the side wall of actuator showing the corrugation profile is shown in Fig. 9(c). For characterization purposes, the actuator was mounted on a metal-coated glass slide, acting as the backside connection, and a needle was used as the front contact. This setup is shown in Fig. 9(d).

IV. Measurement Results

The performance of the single-layer elastomeric out-of-plane actuators were measured using a high-voltage power supply as an actuation source. The actuator movements were monitored under microscope and recorded through a high-speed video frame grabber. Image analyses were performed to calculate the bending movement of the actuator. Fig. 10 shows the tip displacement versus applied voltage for actuators with 3-, 4-, and 5-mm lengths and 1-mm width ($l_1 = 20$ μm, $l_2 = 70$ μm, $t_1 = 40$ μm, and $t_2 = 100$ μm). As can be seen, millimeter-scale actuation was achieved for voltages of less than 1 kV. For the actuator which is 5 mm long and 1 mm wide, the maximum power consumption was 20 μW when actuated with 1 kV (due to leakage through PDMS). The tip deflection of the actuator is within 20% of its simulated value (0.7 versus 0.9 μm; see

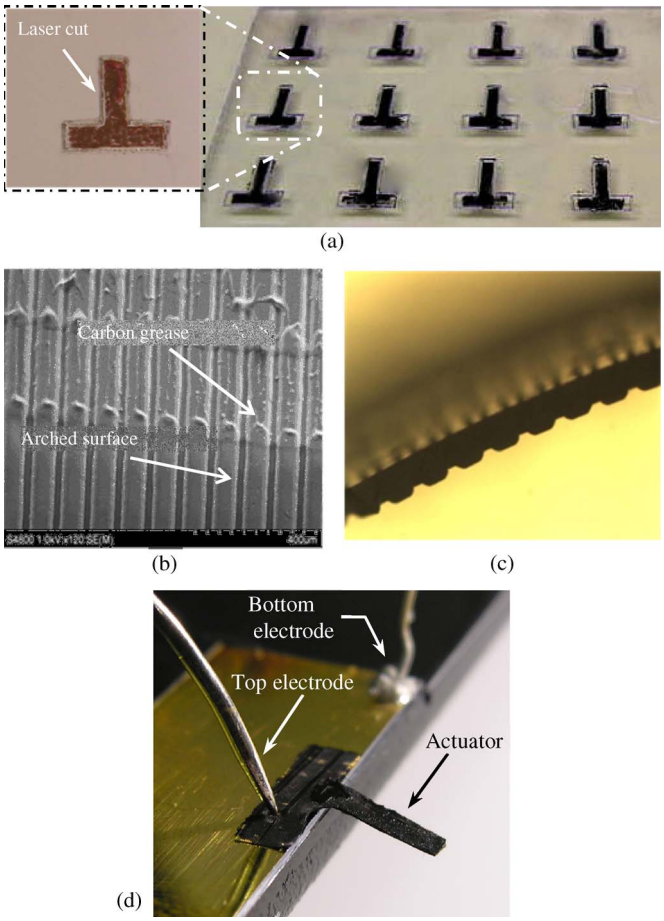

Fig. 9. (a) Batch-fabricated actuators. (b) SEM picture of the actuator showing corrugated surface. (c) Cross-sectional photograph of the actuator. (d) Mounted actuator.

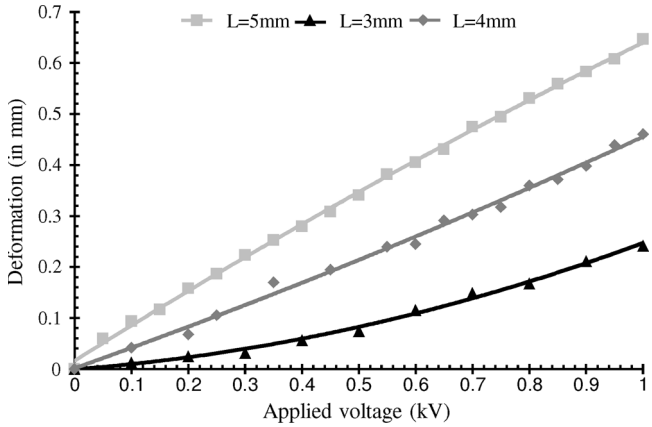

Fig. 10. Displacement versus applied voltage for actuators having 3-, 4-, and 5-mm lengths ($l_1 = 20\ \mu$m, $l_2 = 70\ \mu$m, $t_1 = 40\ \mu$m, and $t_2 = 100\ \mu$m).

Figs. 5 and 10). This error can be attributed to the stiffness of carbon grease electrodes (neglected in the simulation) and the stress induced by the electrical contacts.

It was shown that one can increase the out-of-plane movement of the elastomeric actuators by modulating the stiffness of the structural material [26]. In case of PDMS actuators, this modulation can be simply achieved by controlling the curing-agent-to-the-base ratio. In an attempt to increase the actuator

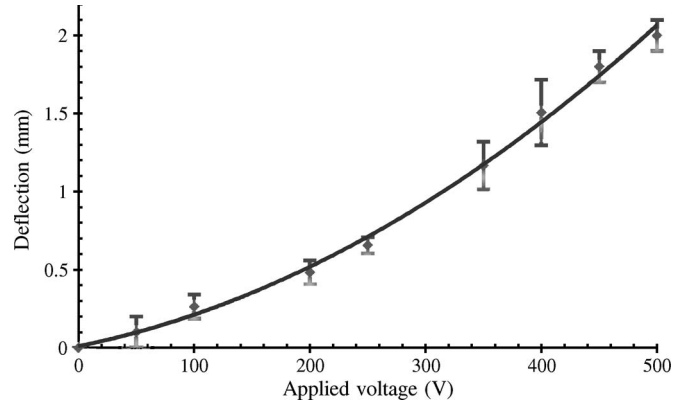

Fig. 11. Tip displacement versus applied voltage. The actuator movement was greatly enhanced by reducing the Young's modulus of the PDMS.

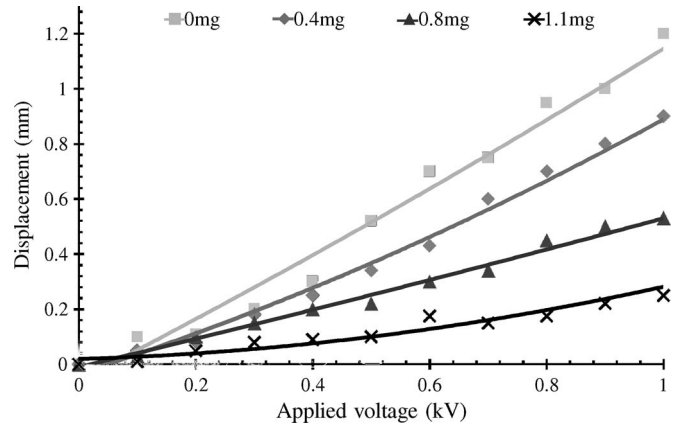

Fig. 12. Deflection versus applied voltage with different masses placed on the tip of the cantilever ($l_1 = 20\ \mu$m, $l_2 = 70\ \mu$m, $t_1 = 40\ \mu$m, and $t_2 = 70\ \mu$m).

out-of-plane displacement, we increased the base-to-curing-agent ratio to 15 : 1. Furthermore, we reduced the thickness of the thin segment to 30 μm, which also increases the tip movement (inset in Fig. 6). Fig. 11 shows the tip displacement versus applied voltage for actuators with 5 mm in length and 1 mm in width ($l_1 = 20\ \mu$m, $l_2 = 70\ \mu$m, $t_1 = 30\ \mu$m, and $t_2 = 70\ \mu$m). As can be seen, millimeter-scale actuation was achieved for voltages of less than 500 V (power consumption of less than 15 μW). However, we should mention that the softened DE actuators are too fragile and difficult to handle.

In order to improve handleability, we fabricated 5-mm-long 1-mm-wide cantilever ($l_1 = 20\ \mu$m, $l_2 = 70\ \mu$m, $t_1 = 40\ \mu$m, and $t_2 = 70\ \mu$m) using a base-to-curing-agent ratio of 10 : 1. For the force measurement setup, we placed different weight on the tip of the actuator and monitored its deflection under microscope using high-speed video frame grabber. By placing different weights of masses (0, 0.4, 0.8, and 1.1 mg of PDMS blocks), the actuator output force at different actuation voltage was measured. As expected, the actuator with heavier mass tends to deflect less, and the actuator with lighter mass tends to deflect more (Fig. 12). The maximum weight that an actuator was capable of moving was 1.5 mg; hence, the maximum output force at zero deflection was calculated to be 15 μN.

The dynamic response of the actuator was evaluated using pulse response and ac input sweep. Similar actuator used

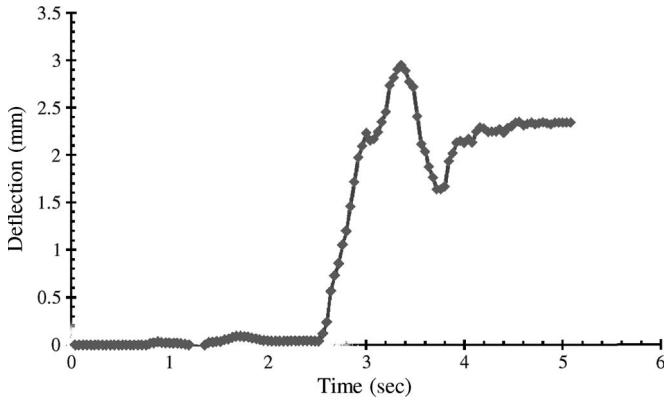

Fig. 13. Time response of the actuator when 1200 V was applied at 0.5 s.

in the previous section (5 mm long, 1 mm wide; $l_1 = 20\ \mu$m, $l_2 = 70\ \mu$m, $t_1 = 40\ \mu$m, and $t_2 = 70\ \mu$m; base-to-curing-agent ratio $= 10:1$) was fabricated and tested. Fig. 13 shows the pulse response of the cantilever when actuated with a 1.5-kV step voltage. Actuator response is slower ($t_r = 0.3$ s) than expected theoretical value from Comsol simulation of the PDMS cantilever without compliant electrode (250 Hz). We believe that this slower response is due to the damping effect of the electrode's mass, the viscoelastic behavior of PDMS and carbon grease, and the limited rise time of the actuation voltage. We also characterized the frequency response using a high-voltage switching supply and found the natural resonant frequency to be $\sim$1 Hz.

Finally, as part of our experimental characterizations, we coated the DE actuators with a thin layer of parylene. This was done in an attempt to investigate the possibility of passivating the electrodes without affecting the performance of the actuators. Electrode passivation is a common concern related to elastomeric actuators and limits their application to gas and nonionic liquid environments [24], [28]–[30]. We coated the cantilevers with 0.1 and 1 μm of parylene and compared the deflection to a noncoated sample [Fig. 14(a)].

As can be seen, even a 100-nm-thick parylene considerably increases the stiffness and decreases the performance. A better method to isolate the electrodes is to physically remove them from the tip of the cantilever (at the expense of a higher actuation voltage). Fig. 14(b) shows a prototype with exposed electrodes residing in a horseshoe-shaped case to prevent the electrode contact with the manipulated object.

V. Discussion

We believe that the described single-layer actuators or an array of them configured in various designs can have interesting applications in MEMS and microrobotics. The actuator performance can be enhanced through careful selection of electrode and elastomeric material. Since the focus of this paper was to present a new design and fabrication process for single-layer DE actuators, we did not attempt to evaluate different materials and their effect on device performance. However, we would like to elaborate on some recent efforts in this area in order to provide a more comprehensive discussion.

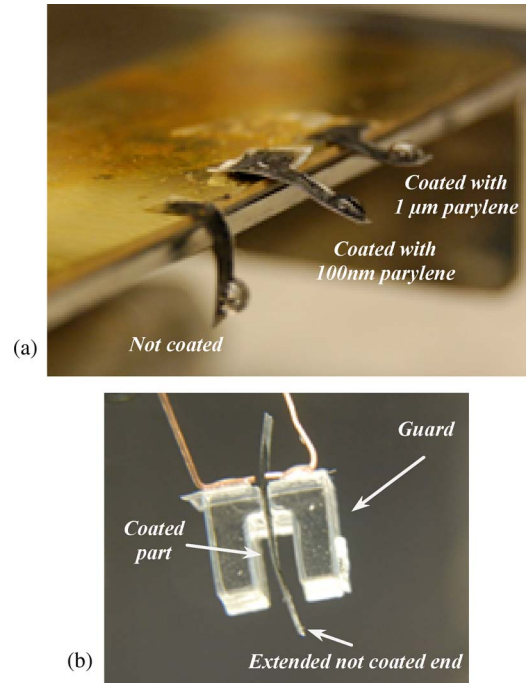

Fig. 14. Isolation of the elastomeric actuator. (a) Parylene coating increases the stiffness and degrades the performance, (b) enclosing the actuator in an acrylic guard.

Carbon grease is the main electrode material used in DE actuators. As mentioned before, although it has some desirable properties such as low deformation resistance, its application in uniform thin layers is challenging (our soft lithography-based stamping simplifies the process by using batch-fabricated PDMS stamps). The performance of the actuator can be improved by replacing the carbon grease electrodes with a more compliant and easier to fabricate/apply electrodes such as thickened electrolyte solution [22], metal-ion-implanted electrodes [28], or elastomers filled with microparticles such as nanotubes, silver, or exfoliated graphite [29]. As for the elastomeric material, several other candidates other than PDMS have been investigated which offer advantages as related to strain, response time, and dielectric breakdown. For example, 3M acrylic elastomers (such as VHB 4910 and VHB F-9473PC) [30], triblock copolymer organogels [30], or polyether-based polyurethane elastomer filled with conductive carbon black [32] can provide more strain per applied electric field. For a faster electromechanical response, Dow Corning silicone (DC 3481) has been used [30]. Another method to enhance the electromechanical performances of the aforementioned actuators is loading the PDMS (or polyurethane elastomer) with high-permittivity microparticles, such as barium titanate, titanium dioxide, or 0.85Pb (Mg1/3Nb2/3)O3–0.15PbTiO3, or blending it with a highly polarizable conjugated polymer such as poly(3-hexylthiophene) [33], [34].

Dielectric breakdown has been a major impediment to wider acceptability of DE actuators. PDMS has the dielectric breakdown of 144 MV/m, while that of acrylic (3M VHB 4910) is 412 MV/m [35]. It should be noted that loading the elastomers with conducting microparticles or blending them with polarizable polymer reduces the dielectric breakdown and limits

the maximum operating voltage [33], whereas nonconducting microparticles result in a higher dielectric breakdown [36].

VI. Conclusion

In conclusion, a batch fabrication process for a single-layer elastomeric actuator based on asymmetric surface profile has been presented. Comsol simulations were performed showing that a more nonuniform profile would generate a greater deflection. Successful fabrication and characterization of three different sizes of actuators with geometry optimized for maximum out-of-plane deflection were presented. There was a reasonable agreement between the measurements and the Comsol simulation results (within 20%). Cantilever beams actuated with voltages as low as 500 V could achieve millimeter-scale out-of-plane displacements. A 5-mm-long actuator was capable of generating 15-μN force when actuated with 500 V and consumed less than 20 μw of power. Although a simple cantilever beam was presented in this paper, similar concept can be applied to several other geometrical designs such as membranes, double-clamped beams, and spiral structures. Applications of this technology can include micropumps, microvalves, and miniaturized manipulators.

Acknowledgment

The authors would like to thank the staff at the Birck Nanotechnology Center, Purdue University, for their assistance in fabrication. The authors would also like to thank Prof. C. Savran for his help with laser micromachining.

References

[1] M. T. Azar, *Microactuators: Electrical, Magnetic, Thermal, Optical, Mechanical, Chemical and Smart Structures*. New York: Springer-Verlag, 1997.

[2] H. Janoch, Ed., *Actuators: Basics and Applications*. New York: Springer-Verlag, 2010.

[3] H. Janoch, Ed., *Adaptronics and Smart Structures: Basics, Materials, Design, and Applications*. NY: Springer-Verlag, 2010.

[4] R. D. Howe and Y. Matsuka, "Robotic for surgery," *Annu. Rev. Biomed. Eng.*, vol. 1, pp. 211–240, 1999.

[5] H. Kim, A. Ucok, and K. Najafi, "Large-deflection stacked multi-electrode electrostatic actuator," in *Proc. 11th Solid-State Sens., Actuator, Microsyst. Workshop*, Hilton Head Island, SC, 2004, pp. 340–343.

[6] J. D. Grade, H. Jerman, and T. W. Kenny, "Design of large deflection electrostatic actuators," *J. Microelectromech. Syst.*, vol. 12, no. 3, pp. 335–343, Jun. 2003.

[7] C. Liu, T. Tsao, G. B. Lee, J. T. S. Leu, Y. W. Yi, Y. C. Tai, and C. M. Ho, "Out-of-plane magnetic actuators with electroplated permalloy for fluid dynamics control," *Sens. Actuators A, Phys.*, vol. 78, no. 2/3, pp. 190–197, Dec. 1999.

[8] Y. A. Pimpin, Y. Suzuki, and N. Kasagi, "Microelectrostrictive actuator with large out-of-plane deformation for flow-control application," *J. Microelectromech. Syst.*, vol. 16, no. 3, pp. 753–764, Jun. 2007.

[9] A. Michael, C. Y. Kwok, K. Yu, and M. R. Mackenzie, "A novel bistable two-way actuated out-of-plane electrothermal microbridge," *J. Microelectromech. Syst.*, vol. 17, no. 1, pp. 58–69, Feb. 2008.

[10] D. Girbau, M. A. Llamas, J. Casals-Terré, X. Simó-Selvas, L. Pradell, and A. Lázaro, "A low-power-consumption out-of-plane electrothermal actuator," *J. Microelectromech. Syst.*, vol. 16, no. 3, pp. 719–727, Jun. 2007.

[11] W. C. Chen, C. C. Chu, J. Hsieh, and W. Fang, "A reliable single-layer out-of-plane micromachined thermal actuator," *Sens. Actuators A, Phys.*, vol. 103, no. 1/2, pp. 48–58, 2003.

[12] Y. Lu and C. J. Kim, "Micro-finger articulation by pneumatic parylene balloons," in *Proc. 12th Int. Conf. Solid State Sens., Actuators Microsyst.*, Boston, MA, 2003, pp. 276–279.

[13] J. Juuti, K. Kordás, R. Lonnakko, V. P. Moilanen, and S. Leppävuori, "Mechanically amplified large displacement piezoelectric actuators," *Sens. Actuators A, Phys.*, vol. 120, no. 1, pp. 225–231, Apr. 2005.

[14] V. Monturet and B. Nogarede, "Optimal dimensioning of a piezoelectric bimorph actuator," *Eur. J. Appl. Phys.*, vol. 17, no. 2, pp. 107–118, Feb. 2002.

[15] F. Carpi, D. D. Rossi, R. Kornbluh, and R. E. Pelrine, Eds., *Dielectric Elastomers as Electromechanical Transducers: Fundamentals, Materials, Devices, Models and Applications of an Emerging Electroactive Polymer Technology*. New York: Elsevier, 2008.

[16] A. O'Halloran, F. O'Malley, and P. McHugh, "A review on dielectric elastomer actuators, technology, applications, and challenges," *J. Appl. Phys.*, vol. 104, no. 7, pp. 071101-1–071101-10, Oct. 2008.

[17] J. S. Plante and S. Dubowsky, "On the properties of dielectric elastomer actuators and their design implications," *Smart Mater. Struct.*, vol. 16, no. 2, pp. s227–S236, Apr. 2007.

[18] R. Kornbluh, R. Pelrine, Q. Pei, R. Heydt, S. Stanford, S. Oh, and J. Eckerle, "Electroelastomers: Applications of dielectric elastomer transducers for actuation, generation and smart structures," in *Proc. SPIE*, San Diego, CA, 2002, pp. 254–270.

[19] F. Carpi, G. Frediani, A. Mannini, and D. D. Rossi, "Contractile and buckling actuators based on dielectric elastomers: Devices and applications," *Adv. Sci. Technol.*, vol. 61, pp. 186–191, 2008.

[20] R. H. Baughman, "Playing nature's game with artificial muscles," *Science*, vol. 308, no. 5718, pp. 63–65, Apr. 2005.

[21] R. Pe1rine, P. S. Larsen, R. Kornbluh, R. Heydt, G. Kofod, and Q. Pei, "Applications of dielectric elastomer actuators," in *Proc. SPIE*, Newport Beach, CA, 2001, vol. 4329, pp. 335–349.

[22] F. Carpi, P. Chiarelli, A. Mazzoldi, and D. D. Rossi, "Electromechanical characterization of dielectric elastomer planar actuators: Comparative evaluation of different electrode materials and different counter loads," *Sens. Actuators A, Phys.*, vol. 107, pp. 85–95, 2003.

[23] R. Kornbluh and R. Pelrine, "High-performance acrylic and silicone elastomers," in *Dielectric Elastomers as Electromechanical Transducers: Fundamentals, Materials, Devices, Models and Applications of an Emerging Electroactive Polymer Technology*. New York: Elsevier, 2008, pp. 33–42.

[24] R. Pelrine, R. Kornbluh, Q. Pei, and J. Joseph, "High-speed electrically actuated elastomers with strain greater than 100%," *Science*, vol. 287, no. 5454, pp. 836–839, Feb. 2000.

[25] R. Pelrine, R. Kornbluh, and G. Kofod, "High-strain actuator materials based on dielectric elastomers," *Adv. Mater.*, vol. 12, no. 16, pp. 1223–1225, Aug. 2000.

[26] T. Maleki, G. Chitnis, and B. Ziaie, "A batch-fabricated laser-micromachined PDMS actuator with stamped carbon grease electrodes," *J. Micromech. Microeng.*, vol. 21, no. 2, p. 027002, Feb. 2011.

[27] R. Pelrine, R. Kornbluh, J. Joseph, R. Heydt, Q. Pei, and S. Chiba, "High-field deformation of elastomeric dielectrics for actuators," *Mater. Sci. Eng., C*, vol. 11, no. 2, pp. 89–100, Nov. 2000.

[28] S. Rosset, M. Niklaus, P. Dubois, and H. R. Shea, "Mechanical characterization of a dielectric elastomer microactuator with ion-implanted electrodes," *Sens. Actuators A, Phys.*, vol. 144, no. 1, pp. 185–193, 2008.

[29] M. Kujawski, J. D. Pearse, and E. Smela, "Elastomers filled with exfoliated graphite as compliant electrodes," *Carbon*, vol. 48, no. 9, pp. 2409–2417, Aug. 2010.

[30] S. Michel, X. Q. Zhang, M. Wissler, C. Lowe, and G. Kovacs, "A comparison between silicone and acrylic elastomers as dielectric materials in electroactive polymer actuators," *Polym. Int.*, vol. 59, no. 3, pp. 391–399, Mar. 2010.

[31] R. Shankar, A. K. Krishnan, T. K. Ghosh, and R. J. Spontak, "Triblock copolymer organogels as high-performance dielectric elastomers," *Macromolecules*, vol. 41, no. 16, pp. 6100–6109, Aug. 2008.

[32] K. Wongtimnoi, B. Guiffard, A. Bogner-Van de Moortèle, L. Seveyrat, C. Gauthier, and J.-Y. Cavaillé, "Improvement of electrostrictive properties of a polyether-based polyurethane elastomer filled with conductive carbon black," *Composites Sci. Technol.*, vol. 71, no. 6, pp. 885–892, Apr. 2011.

[33] G. Gallone, F. Galantini, and F. Carpi, "Perspectives for new dielectric elastomers with improved electromechanical actuation performance: Composites versus blends," *Polym. Int.*, vol. 59, pp. 400–406, 2010.

[34] F. Carpi, G. Gallone, F. Galantini, and D. D. Rossi, "Silicone-poly (hexylthiophene) blends as elastomers with enhanced electromechanical transduction properties," *Adv. Funct. Mater.*, vol. 18, no. 2, pp. 235–241, Jan. 2008.

[35] P. Brochu and Q. Pei, "Advances in dielectric elastomers for actuators and artificial muscles," *Macromol. Rapid Commun.*, vol. 31, no. 1, pp. 10–36, Jan. 2010.

[36] G. Kofod, H. Stoyanov, M. Kollosche, S. Risse, H. Ragusch, D. N. McCarthy, R. Waché, D. Rychkov, and M. Dansachmüller, "Molecular level materials design for improvements of actuation properties of dielectric elastomer actuators," in *Proc. SPIE*, 2011, vol. 7976, pp. 79760J-1–79760J-12.

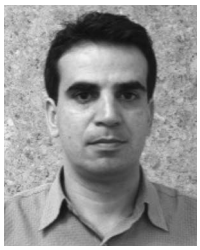

Teimour Maleki (M'09) received the B.Sc. degree in biomedical engineering from Amirkabir University of Technology, Tehran, Iran, in 2000, the M.Sc. degree in electrical engineering from the University of Tehran, Tehran, in 2003, and the Ph.D. degree in electrical engineering from Purdue University, West Lafayette, IN, in 2010.

He is currently a Research Assistant Professor with the Birck Nanotechnology Center, Purdue University. His focus is on developing microelectromechanical-systems-enabled point-of-care systems for healthcare and implantable microdevices.

Girish Chitnis received the B.S. degree in mechanical engineering from the Indian Institute of Technology Bombay, Mumbai, India, in 2007. In 2007, he joined Purdue University, West Lafayette, IN, where he is currently working toward the Ph.D. degree in engineering.

His research interests are related to microelectromechanical systems and their biomedical applications.

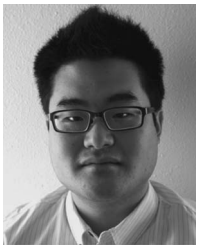

Albert Kim was born in Delaware in 1983. He received the B.S. and M.S. degrees from Purdue University, West Lafayette, IN, where he is currently working toward the Ph.D. degree in electrical engineering.

He is currently a member of a research team, ZBML, that is developing biomedical devices at the Birck Nanotechnology Center, Purdue University. His interests include design and fabrication of implantable devices for energy scavenging from acoustic waves and liquid-based microtransponders.

Babak Ziaie (A'95–M'00–SM'07) received the Ph.D. degree in electrical engineering from the University of Michigan, Ann Arbor, in 1994.

From 1995 to 1999, he was a Postdoctoral Fellow and an Assistant Research Scientist with the Center for Integrated Microsystems, University of Michigan. He subsequently joined the Electrical and Computer Engineering Department, University of Minnesota, Minneapolis, as an Assistant Professor (1999–2004). Since January 2005, he has been with the School of Electrical and Computer Engineering, Purdue University, West Lafayette, IN, where he is currently a Professor. His research interests are related to the biomedical applications of microelectromechanical systems and microsystems (bioMEMS).